

This article was downloaded by: [University of Vermont]

On: 22 April 2014, At: 12:14

Publisher: Taylor & Francis

Informa Ltd Registered in England and Wales Registered Number: 1072954 Registered

Downloaded from <https://www.cambridge.org/core> at <https://www.cambridge.org/core> on 10 Jun 2018 at 10:52:11, subject to the Cambridge Core terms of use, available at <https://www.cambridge.org/core/terms>. <https://doi.org/10.1017/S0022296518000000>

A new approach for forest decline assessments: maximizing detail and accuracy with multispectral imagery

Jennife Ponikvar *

Rubenstein School of Environment and Natural Resources, University of Vermont, Burlington, VT, USA; USDA Forest Service, Northern Research Station, Burlington, VT 05405, USA

(Received 27 June 2013; accepted 2 March 2014)

Remote sensing of forest condition is typically based on broadband vegetation indices to quantify canopy condition. More detailed and accurate assessment has been demonstrated using narrow band sensors, although their more limited image availability. While differences in sensor capabilities are obvious, the potential of high resolution multispectral imagery may be able to detect subtle canopy composition if a new calibration approach is considered. This involves three major changes to additional decline assessment: (1) calibration of high resolution field measurements, (2) consideration of narrow band derived indices adapted for broadband calibration, and (3) a multispectral calibration model. Testing this approach on Landsat-5 (TM) imagery in the Catskills, NY, USA, a fire-emissions vegetation model ($r^2 = 0.621$, RMSE 0.403) based on a unique combination of vegetation indices (green canopy chlorophyll, carotenoid, green leaf area, and a vegetation index) to quantify broadband forest condition accuracy. When compared to a standard method, high resolution predicted decline accuracy 42% improved (65% accuracy (10-class), and 100% accuracy (5-class)). This approach is a significant improvement over common vegetation indices such as NDVI ($r^2 = 0.351$, RMSE = 0.500, 10-class accuracy = 60%, and 5-class accuracy = 74%). The evaluation suggests high resolution on a single common vegetation index is a forest condition measurement limitation and a more detailed multispectral image is recommended for more effective monitoring of forest decline considering the high-resolution approach to decline prediction in order to maximize information and accuracy obtainable with broadband sensors.

1. Introduction

Multispectral remote sensing sensors such as Landsat have been used for decades to assess a wide range of vegetation biological parameters. The use of vegetation indices (VI) based on the unique reflectance characteristics of vegetation is a simple and well-understood technique. The most common include the vegetation index (RVI) (Peacock and Miller 1972) and NDVI (Rouse et al. 1974). No matter the name of common indices to change in background properties, another class of indices is designed to account for soil and atmospheric background variation (e.g. soil adjusted vegetation index (SAVI) – (Keane, Morgan, and Menakis 1994) and forest SAVI (TSAVI) (Zhang and King 1997)). In forest health applications, these indices are typically used to identify broad categories of forest condition (primarily changes in defoliation class) for a single species of interest. For example,

*Email: Jennife.ponikvar@uvm.edu | Td(indice).(ponikvar.58.20(0m5f58.2511-0n il131358.866-0.397lea.866-0.34[(Vc)5

Lambe et al. (1995) used Landsat imagery to evaluate the percentage of damage in North America in 1985; Role and Lathrop (2002) predicted foliar loss of hemlock defoliation in 1982; Wang, Li, and Haihoo (2007) quantified the percentage of oak decline in response to the drought of 1999 in 76% accuracy; and Aerial et al. (2006) evaluated a penicillium, mold, and other damage in 70% accuracy.

While this approach may be useful for a general estimate of change in canopy, limiting prediction of a small number of canopy classes lacks the detail necessary to detect early, moderate decline symptoms or monitor long-term end of time. Addressing this limitation of canopy classification of forest condition, Tomend et al. (2012) used Landsat imagery to monitor canopy defoliation, quantified a change in common vegetation indices, between pre-moist defoliation and non-defoliation years. Their final model is able to estimate defoliation, with RMSE = 14.9% and cross-validation $r^2 = 0.805$. While this represents an improvement over typical broad canopy classification of forest condition, it still faces some of the same issues in relation to homogeneous deciduous and

In contrast to the typical effect, narrow band hyperspectral sensors have been used to quantify a range of forest biophysical, structural, and process-based (e.g. productivity) characteristics. The accuracy of these effects can be attributed to both the narrow spectral signal of key biophysical attributes that can be detected in narrow bands and the analytical calibration possible in many configurations. The development of narrow band indices is typically based on laboratory measurements of known properties of the target biophysical parameter (such as chlorophyll content, chlorophyll fluorescence, leaf area content) are linked to a parameter 'intrinsic' to the band. This has led to the development of indices to quantify chlorophyll content (Gitelson and Merzlyak 1996), photosynthetic activity (Caetano 1998; Caetano, Cibulka, and Miller 1996), and moisture content (Adam et al. 2000) on a global scale. Hyperspectral sensors have also been used to quantify forest decline. Ponton, Halle, and Martin (2005a) used NASA's AVIRIS sensor to predict hemlock needle loss (Adelges tsugae)-induced decline in eastern hemlock (*Tsuga Canadensis*) and used Spectral VNIR sensor to locate incipient needle loss (Agrilus planipennis) infection in a *Fraxinus* spp. (Ponton et al. 2008).

In an attempt to merge the information and detail from hyperspectral imagery with the widespread availability of multispectral imagery, a forest decline assessment methodology proposed hinges on these two components. First, the characteristic absorption of forest condition from image calibration is a de-aliased, continuous, unimodal decline along the canopy edge gradient of vegetation symptoms (Ponton and Halle forthcoming). This is a departure from the broad classes of canopy condition typically used for forest decline.

Second, the condition of a forest of vegetation indices, including narrow band-derived indices, is used only in the hyperspectral sensor. Because the narrow band indices are based on the same spectrum as the biophysical characteristic of vegetation, the characteristic of narrow band attributes, especially unlikely to have a broad band sensor to quantify the specific parameter in the same precision as a narrow band sensor. However, it is possible to have a calibration 'equivalent' of narrow band-derived indices (see Section 2.2) could capture the characteristic of vegetation that may be useful in decline assessment.

The final component of the proposed approach in order to develop a multi-scale prediction model has combined a series of indices, which can be used in combination of

proposed approach can provide a more detailed and accurate assessment of forest condition than models based on additional indices.

2. Methods

2.1. Field methods

This study builds on previous research (Ponikvar, Halle, and Martin 2005a, 2005b) in the Catskill Mountain region of NY (Figure 1). The Catskill region is selected based on the convergence of many forest types, range of species composition, and elevational gradients. It is also a key area for the New York City Metropolitan Area, making the function and condition of its forested areas a high priority. In 2007, forest health monitoring plots (Figure 1) were established across the region spanning a range of forest conditions, species, and life characteristics. This included plots dominated by maple (*Acer*), birch (*Betula*), pine (*Pinus*), hemlock (*Tsuga*), oak (

aken in the field, percentage fine twig dieback, and percentage live crown and crown vigor. The following Forest Health Monitoring guideline (USDA 1997). Additional measurements of percentage needle loss are included for hemlock, while percentage defoliation is a subject area covered in 10% increments for hardwood.

In order to estimate the information from each of the measurements in one continuous, annual decline analysis, each available area is divided into a 0-10 scale based on species-specific population distribution from one to ten areas of field sampling across the northern USA (available from the author upon request). Using percentage based on a minimum of 100 individual and spanning a full range of possible conditions, from optimal health to dead, each decline analysis is made and analyzed by species. Percentage assignments for all measured decline components are then assigned for each tree to produce a continuous annual decline analysis for each tree. Plot-level conditions for image calibration are calculated as the average of all tree assigned by species percentage based areas. This plot-level assigned average percentage coefficient is multiplied by 10 to force a 0-10 decline scale. To exemplify this process, field measurements, analyzed percentage, and final decline analysis are presented in [Table 1](#).

The resulting plot-level decline annual analysis ranged from 2 to 5.97, with a mean of 4.02 and standard deviation of 0.68. Combining multiple measurements in one annual decline analysis provides a comprehensive, continuous measurement for more detailed image calibration, from each individual function in photoconductive function (chlorophyll fluorescence) or indication of imminent death.

Table 1. An example of the plot, mma decline a ing calo la ion fo a plo i h fi e canop dominan ee ep e en ing h ee diffe en pecie . Field-measured al e (FMV) a e fi no ma ed o a pecie -ba ed pe cen ile co e (SBP) ba ed on a da aba e of o e 2000 ee f om ac o he no hea . Pe cen ile fo all a iable a e a e aged fo each ee and hen b pecie o ha a plo -le el a e age can be eigh ed b pecie pe cen age ba al a ea. Thi final eigh ed a e age pe cen ile co e i hen m. l iplied b 10 fo he 0-10 decline cale.

Field mea t, emen	Acer rubrum-1		Acer rubrum-2		Acer saccharum-1		Fagus grandifolia-1		Fagus grandifolia-2	
	FMV	SBP	FMV	SBP	FMV	SBP	FMV	SBP	FMV	SBP
C o n i go.	1	0.21	2	0.60	1	0.24	1	0.23	1	0.23
Pe cen age dieback	5	0.28	10	0.55	5	0.36	5	0.29	5	0.29
F Fm	0.79	0.06	0.82	0.76	0.82	0.69	0.79	0.19	0.86	0.93
Pe cen age li e c o n	0.61	0.81	0.60	0.80	0.44	0.35	0.67	0.84	0.61	0.73
PI	1.99	0.05	2.84	0.19	2.17	0.12	1.52	0.10	2.60	0.17
Tree average	0.28		0.58		0.35		0.33		0.47	
Species average	0.43		0.43		0.350,98003Tm[(T)5a(average)]TJ28.21955Td(0.43)TJ3.8411Td(0.35)TJ3					

vegetation characteristics. Equivalence is used for an index of the vegetation - band equivalent calculation contained within the Landsat spectral angle, and all available equivalent indices calculated within the band. A single angle of the Landsat equivalent could be calculated, considering the chlorophyll content index proposed by Da (1998). This narrow band index is calculated as $(R_{672} \text{ nm} / R_{550} \text{ nm})$. Considering the Landsat-5 (TM) band 2 angle from 520 to 600 nm and band 3 measured between 630 and 690 nm, I calculated a broadband equivalent of Da'

Table 2. Spearman's Rho correlation between field-measured δ_{O} and δ_{C} of vegetation indices.

Tadiational indice	Spearmann' p	Indefo mla	Referece
AI	0.0758	B3/B1	Wol e and To n end (2011)
DVI	-0.1541	[B4]-[B3]	Jo dan (1969)
EVI	-0.215**	2.5 (([B4]-[B3])/([B4] + (6 [B3])-(7.5 [B1]) + 1))	H, e e e al. (2002)
GI	-0.1453	[B2]/[B3]	Si anpillai e al. (2006)
MIR	-0.2343***	B5/B7	El idge and L on (1985)
MSAVI	-0.1541	0.5 (2 [B4] + 1-(Sq (((2 [B4] + 1) (2 [B4] + 1))))-(8 ([B4]-[B3])))	Qi e al. (1994)
MSI	0.3323***	B5/B4	Rock e al. (1986)
NDII 5	-0.3214***	(B4-B5)/(B4 + B5)	Ha di k, Klema , and Sma (1983)
NDII 7	-0.2788***	(B4-B7)/(B4 + B7)	H, n and Rock (1989)
NDVI	-0.1911**	([B4]-[B3])/([B4] + [B3])	Ro e e al. (1974)
OSAVI	-0.1993**	([B4]-[B3])/([B4] + [B3] + 0.16)	Rondea , S e en, and Ba e (1996)
RAI	-0.2891***	B4/(B3 + B5)	AZ ani and King (1997)
RDVI	-0.1921**	Sq (((([B4]-[B3])/([B4] + [B3])) ([B4]-[B3])))	Ro , jean and Be on (1995)
RVI	-0.0307	[B4]/[B3]	Pea on and Mille (1972)
SARVI	0.1486	1.5 ((([B4]-[B3]-([B1]-[B3])))/([B4]-([B3] + ([B1]-[B3]) + 0.5))))	H, e e, k, ice, and Li. (1994)
SAVI	-0.1763*	1.5 ((([B4]-[B3])/([B4] + [B3] + 0.5)))	H, e e (1988)

Na o band indice	Speamann' p	Na o band	B oadband eq. i alen	Referece
Aoki	0.0286	R ₅₅₀ /R ₈₀₀	B2/B4	Aoki, Yabuki, and Totsuka (1981)
BNa	-0.1429	R ₈₀₀ /R ₅₅₀	[B3]/[B2]	B, chman and Nagel (1993)
CMS	0.1911**	R ₆₉₄ /R ₇₆₀	B3/B4	Ca e (1994)
CSe	0.3237**	R ₆₉₄ /R ₄₂₀	B3/B1	Ca e (1994)

(Continued)

Table 2. (Continued).

Na o band indice	Spea man' p	Na o band	Inclg fo m. la	B oadband eq. i alen	Refere nce
Da	0.0584	$R_{672} (R_{550} R_{708})$	$[B3] [B2] [B3]$		Da (1998)
Da b	0.0938	R_{750}/R_{550}	$[B3]/[B2]$		Da (1998)
Flo	-0.2343**	FD_{690}/FD_{735}	$([B4]-[B2])/([B5]-[B3])$		Mohammed, Binder, and Gillies (1995)
Gi c	-0.0057	$1/R_{700}$	1/B3		Gi el on, M el ak, and Chi k no a (2001)
GM	0.1606	R_{750}/R_{550}	$[B4]/[B2]$		Gi el on and M el ak (1994)
MCARI1	0.1806*	$1.2 ((2.5 (R_{800}-R_{670}))-(1.3 (R_{800}-R_{550})))$	$1.2 (2.5 (B3))-(1.3 (B4-[B2]))$		Hab o dane e al. (2004)
MCARI2	-0.2604***	$1.5 \times ((2.5 \times (R_{800}-R_{670}))-(1.3 \times (R_{800}-R_{550}))) / (Sqr(((2 \times R_{800}+1) \times (2 \times R_{800}+1))))-(6 \times R_{800}-(5 \times (Sqr(R_{670}))-0.5)))$	$1.5 (2.5 (B4-[B3]))-(1.3 (B4-[B2])) / (Sqr(((2 [B4] + 1) (2 [B4] + 1))))-(6 [B4]-[B3]))-(0.5)))$		Haboudane et al. (2004)
MND705	-0.1166	$(R_{750}-R_{705})/(R_{750} + RR_{705} + 2R_{445})$	$(B4)-B3)/(B4 + B3 + (2 B1))$		Sim and Gamon (2002)
MSR	-0.0307	$(R_{800}-R_{678})-1)/(Sqr((R_{800}/R_{670} + 1))$	$(([B4]-[B3])-1)/(Sqr([B4]/[B3] + 1))$		Chen (1996)
MSR705	0.0407	$(R_{750}-R_{445})/(R_{705}-R_{445})$	$(B4)-[B1])/([B4] + [B1])$		Sim and Gamon (2002)
MTVI	-0.1698*	$1.2 ((1.2 (R_{800}-R_{550}))-(2.5 (R_{670}-R_{550})))$	$1.2 (1.2 (B4-[B2]))-(2.5 (B3-[B2]))$		Hab o dane e al. (2004)
MTVI2	-0.2853***	$(1.5 \times ((1.2 \times (R_{800}-[R_{550}]))-(2.5 \times (R_{670}-[R_{550}])))/(Sqr(((2 \times [R_{800}] + 1) \times (2 \times [R_{800}] + 1)-(6 \times [R_{680}-R_{430})/(R_{680} \times R_{430}))$	$(1.5 ((1.2 (B4-[B2]))-(2.5 (B3-[B2])))/(Sqr(((2 [B4] + 1) (2 [B2])))/(Sqr(((2 [B4] + 1) (2 [B4] + 1))-(6 [B4]-[B3]))-(0.5))))$		Hab o dane e al. (2004)
NPCI	0.2837***	$(R_{680}-R_{430})/(R_{680} \times R_{430})$	$(B3-B1)/(B3 + B1)$		Pe e la e al. (1994)
PSSRa	-0.0307	R_{600}/R_{680}	$[B4]/[B3]$		Blackb n (1998)
SIPI	0.393***	$(R_{803}-R_{445})/(R_{800}-R_{680})$	$(B4)-[B1])/([B4]-[B3])$		Pe u el as, Baret, and Filella (1995)
SRPI	-0.2426**	R_{430}/R_{680}	$[B1]/[B3]$		Pe e la e al. (1993)
TVI	-0.1654*	$0.5 (120 (R_{avg760 to 800}-R_{avg530 to 570}) - (200 (R_{avg650 to 680}-R_{avg530 to 570}))$	$0.5 (120 (B4-[B2]))-200 (B3-[B2]))$		B o ge and Leblanc (2001)
VogB	-0.2544***	FD_{715}/FD_{705}	$(B4)-[B3])/([B5]-[B4])$		Vogelmann, Rock, and Mo (1993)

No e : *indica e p < 0.1, **p < 0.05 and ***p < 0.01. R deno e eflec ance a he pecified a eleng h, FD deno e he fi de i a i e cen e d a he pecified a eleng h, and B deno e he pecified Land a -5 (TM) band. Va iable in bold e e eled e d fo he final m. l i a i a e model.

band on a ratio between normalised reflectance at 450 nm and chlorophyll *a* concentration, and reflectance at 680 nm and chlorophyll *b*. SIPI characteristics are the population of chlorophyll pigments (Peñuela, Bae, and Filella 1995). Because vegetation optically manifests a reduction in chlorophyll pigments, change in the ratio between pigments has been used to detect chlorophyll decline symptoms in vegetation (Peñuela et al. 1994).

The long-wavelength-derived index correlates with the maximum decline metric of the maximum index (MSI, $r = 0.332$) (Rock et al. 1986). A comparison of band 5 and 4, the index makes use of the difference between absorption in band 5, in combination with the near-infrared NIR band. MSI has been significantly correlated with measured concentration in multiple species (Cho and Skidmore 2006; Hu and Rock 1989; Hai, Ban, and Baird 2006). In 2007 there were no documented periods of abnormal conditions over the study area (following season peak in abnormality). However, availability is a common agent in the Cañon, due to the presence of deep rain and oak, halving soil.

Another long-wavelength index significantly correlated with the maximum decline metric of the normalised difference index (NDII5, $r = -0.321$; Hai, Klemm, and Sma 1983). Although band 5, NDII5 increases with increasing canopy concentration and has been significantly correlated with vegetation concentration (Hai, Klemm, and Sma 1983) and the decrease in agricultural crop (Jackson et al. 2004). In contrast, Hu and Rock (1989) concluded that indices derived from near-infrared and mid-infrared reflectance were not sensitive enough to estimate vegetation. Because equal area hickory correlates with leaf area index, area index and NDII5 are also a proxy for leaf area and canopy density estimates (Hu and Rock 1989). In this study NDII5 has also been used for canopy monitoring, including imbalanced action in energy (Sosa, Roberts, and Cochane 2005) and potential fire damage (Wang et al. 2010).

Much of Cañon's work has focused on identifying key narrow-band indices for vegetation concentration and estimation of chlorophyll concentration (Cañe 1994; Cañe, Cibulka, and Mille 1996; Cañe and Knapp 2001; Cañe and Mille 1994; Cañe and Spieing 2002). Although designed for narrow-band field and laboratory environments, one of the indices has been developed for the decrease in area of a significant correlation with the maximum decline index ($r = 0.3237$) (Cañe 1994) in the long-wavelength form. Reflected over the Cañon area (CS_c), the comparison of the area index in the NIR and CS_c has been used to detect differences in vegetation concentration and vegetation species and agents (Cañe 1993, 1994). This comparison reflects the presence of a reduced or induced inhibition of chlorophyll production (Cañe 1993). It has also been identified as a potential index for the decrease in chlorophyll and concentration index of vegetation in the form of the area index of vegetation collapse during the event (Cañe and Mille 1994).

3.2. Decline predictive model

Considering the field-measured maximum decline metric in multiple species

Table 3. The final multiple linear regression model for estimating Land a-5 (TM) image of the Catskill, NY. Predictable each combination of variables information related to biophysical characteristics of vegetation.

Term	Parameter estimate	Abundance feature	Reference
Intercept	-51.763		
B5	0.946	Canopy moisture content, leaf area index, and total biomass	Vieira et al. (2003)
Aoki	0.706	Chlorophyll content	Aoki, Yabuki, and Tokka (1981)
MCARI2 (modified chlorophyll absorption index)	-0.236	Green leaf area index	Haboudane et al. (2004)
SIPI (structural index independent pigment index)	54.536	Carotenoid: chlorophyll	Peterson, Baret, and Filella (1995)
Flo (chlorophyll fluorescence index)	0.451	Chlorophyll fluorescence	Mohammed, Binde, and Gillie (1995)

calibration, I used a modified stepwise regression model to identify the best predictive model. The resulting five-term model is based on a combination of narrow-band derived indices and Land a-5 (TM) reflectance band 5 (Table 3). Each of the available vegetation indices decline rapidly, including chlorophyll content, ratio of chlorophyll to carotenoid, canopy density, moisture content, and chlorophyll fluorescence. Because each predictive variable is associated with a specific, well-related biophysical characteristic, correlation between a variable and a negligible (multiple model VIF = 3.9).

Across all different periods, the resulting equation is able to predict the 0-10 summer decline in high accuracy than additional indices. While this equation holds across periods, the evidence for a high accuracy (high productivity and increase in decline) to be under- and over-predicted, respectively.

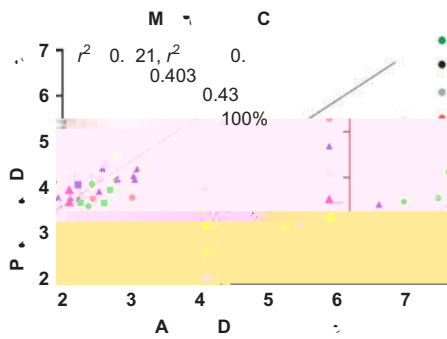


Figure 2. The final 5-term model is able to predict the 0-10 summer decline in high accuracy than additional indices. While this equation holds across periods, the evidence for a high accuracy (high productivity and increase in decline) to be under- and over-predicted, respectively.

Downloaded by [University of Vermont] at 12:14 22 April 2014

errors included in model prediction are typically minor and do not exceed what should be necessary to account for a large category of force conditions.

ell μ ha the image p e-p oce ing and a mo phe ic co ec ion comple ed a a pa of hi μ d i μ fficien o minim μ e hi po en ial in e fe ence ac o image a ea and image acq i i ion da e .

A fl o e cence ind μ (Flo) a al o e ained in he final p edic i e model. Chlo oph ll fl o e cence can be μ ed a an indi ec mea μ e of ed c ion in chlo oph ll μ c μ e and fl nc ion ha picall oca in he ea lie age of ege a ion e (S a e , S i a a a, and Go indjee 1995; S a e and T imilli-Michael 2001). In field calib a ion mea μ emen , I μ ed a chlo oph ll fl o e cence me e o q an if hi ea l e mp om a he pe fo mance ind μ (PI). PI i an e ima e of ho efficien l a leaf can ab o b and μ e ligh hile pe fo ming pho o n he i b q an if ing he fl o e cence e pon e of lea e (S a e and T imilli-Michael 2001). S ch chlo oph ll fl o e cence me ic a e ho n o be an efficien ool o de ec di μ bance and damage o pho o n he ic appa a μ and fl nc ion (Lich en hale 1992).

To cap μ e he chlo oph ll fl o e cence e pon e μ ing eflec ance pec a, Mohammed, Binde , and Gillie (1995) de igned a na o band a io be een fi de i a i e a F₆₉₀ and F₇₃₅ nm (Flo). Simila combina ion of na o band a eleng h in he e egion ha e been μ ed o q an if fl o e cence (Lich en hale and Babani 2000; B chmann and Lich en hale 1999; Gi el on, B chmann, and Lich en hale 1999; Lich en hale e al. 1998; D'Amb o io, μ abo, and Lich en hale 1992; Hak, Lich en hale , and Rinde le 1990; Rinde le and Lich en hale 1988). Rega dle of he diffe ence in pecific na o band loca ion, each of he e p opo ed fl o e cence me ic can be modified fo b oadband cal μ la ion a Land a -5 (TM) (B4-B2)/(B5-B3) (Table 2). Bec μ e of he di ec mea μ emen of fl o e cence in he field calib a ion da a, i i no μ p i ing ha a chlo oph ll fl o e cence ind μ a e ained in he final p edic i e model. I i likel ha hi ind μ con ib e p edic i e po e a he lo end of he μ mma decline a ing, he e ed c ion in chlo oph ll μ c μ e and fl nc ion a e he dominan e mp om .

Ba ed on a imple a io be een na o band eflec ance a 550 and 800 nm, he Aoki ind μ (Aoki, Yab ki, and To μ ka 1981) a de igned a a non-de μ c i e me hod fo e ima ing leaf chlo oph ll concen a ion in m l iple ag i μ l μ al pecie . Blackb n and Seele (1999) al o linked he Aoki ind μ o o al chlo oph ll concen a ion in a labo a o μ d of decid μ lea e . Ho e e , he fo nd an q ponen ial ela ion hip, indica ing ha he ind μ ma become in en i i e a high chlo oph ll concen a ion . Sa μ a ion of he Aoki ind μ o ld be q pec ed a he lo end of he decline a ing cale. Con ide ing hi po en ial in en i i i o eal decline, i i he efo e no μ p i ing ha Aoki a no fo nd o be a ignifican linea co ela e i h he μ mma decline a ing. B a a p edic o in a m l i a i a e model, Aoki ma con ib e ignifican l o diffe en ia ing he mo e e e e decline mp om o hich he o he p edic o a iable (SIPI and Flo) a e no a en i i e .

Simila l , MCARI2 i an ind μ mo e en i i e o la e mp om of decline μ ch a defolia ion and canop hinning h o gh e ima ion of geen leaf a ea ind μ (LAI). De eloped b Hab μ dane e al. (2004), MCARI2 i a modified a ian of pec al ind μ o ginall in ended o mea μ e pho o n he icall ac i e adia ion ela ed o chlo oph ll ab o p ion. The goal of hi modifica ion a o c ea e an ind μ le en i i e o chlo oph ll effec , mo e e pon i e o geen LAI a i a ion , and mo e e i an o oil and a mo phe e effec (Hab μ dane e al. 2004). MCARI2 demon a e a clea linea ela ion hip i h leaf a ea ind μ , i ho a p on μ ced change of he lope o a μ a ion a high e chlo oph ll concen a ion (W μ e al. 2010). Bec μ e ed c ion in leaf a ea ind μ a e mo no iceable hen decline incl μ de mo e e e e le el of dieback,

ence, and general canopy thinning, is likely to have MCARI2 index indicating a period of decline.

Wave number band provided in graph are characteristic, while number of leaf measured in the field calibration data, provided an indication of canopy condition. Because many of the species in the region, such as annual dogwood and hickory, are in loss of vigor due, while others such as hemlock, loblolly pine and beech bark disease impede overall condition of the forest, it is not surprising that wave number band region is included in the final model. Selected leaf area content picked up in the mid-IR from 1400 to 2500 nm (covered in part Landsat-5 (TM) band 5 at 1550 to 1750 nm) due to leaf degradation and the accompanying decreased absorption area (Carter 1993; Hu and Rock 1989; Jensen 1996). The wave number index has made use of the canopy content band 5 for canopy area content. However, in the final stepwise regression model, single band provided a unique contribution to decline of the canopy. More complex multi-wave number indices based on multiple bands. A wide range of canopy content, the disease has affected Landsat-5 (TM) band 5 of a forest biomass, species diversity, density, and leaf area index in optical forest (Vieira et al. 2003).

3.3. Model comparison to traditional indices

In order to compare how the multiple area model compares to the more common approach of using individual indices, calibration of the complete forest of the more common additional broadband indices. The most accurate broadband index is a NDVI ($r^2 = 0.351$, RMSE = 0.501). This is a notable departure from the accuracy obtained using the multiple area model derived above ($r^2 = 0.621$, RMSE = 0.403). However, it is important to consider that NDVI is typically used to ignore broad classes of canopy condition, as opposed to a continuous decline in NDVI accuracy as a class variable (10-class = 60%, 5-class = 74% accuracy) is consistent with previous studies using Landsat-5 to evaluate forest decline (Lambert et al. 1995; Rolle and LaHoop 2002; Wang, Lu, and Haihoo 2007; Annual et al. 2006), with 75%, 82%, 76%, and 70% accuracy respectively. Therefore, as a class variable, the multiple area model provided the most accurate (10-class = 65%, 5-class = 100% accuracy) than any previous effort using NDVI alone.

It is likely that NDVI does not predict the maximum decline among all the multiple area model, because of the inclusion of the total decline component (fluorescence) in field calibration measurements. NDVI is known to vary in dense canopy (Wang et al. 2010) and may not be able to distinguish the total response of degraded photosynthesis function in canopy. However, the relationship between the index and the difference in NDVI across species confirmed the significant inter-species difference.

To examine how multiple area model differs from additional multiple area models across a landscape, I applied both the NDVI and multiple area model to all pixels in the study region (Figure 3). While both NDVI and the multiple area model identify 'hot spots' of forest decline, the broader area of regional canopy condition and detail contained the inter-species difference between the two. Based on field data, NDVI over-predicted all plots in the 0-3 decline maximum range, even all logging health and high forest in total decline. This is evident in the NDVI-predicted decline coverage (Figure 3).

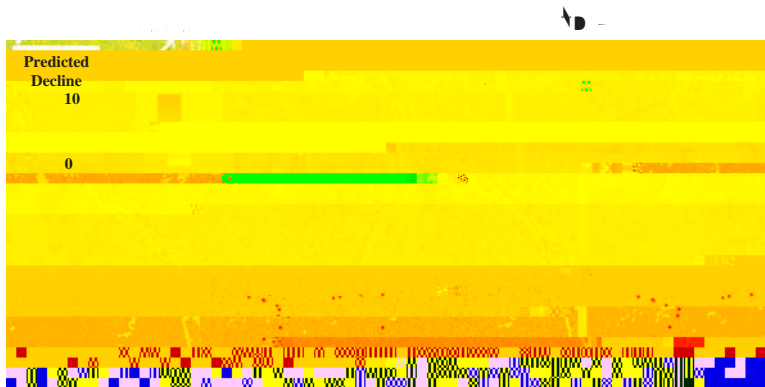


Figure 3. A comparison of the multi-scale and NDVI prediction of forest condition at Woodland Valle (~UTM WGS84 556300 E 4656000 N), a region of even hemlock-sitka spruce forest. While both models detect similar location of moderate decline, NDVI is not able to discriminate between healthy canopy from those in the early stage of decline. As a result, the NDVI assessment of the region suggests higher average decline condition across the region than the multi-scale model and field measurements.

pixels than the multi-scale model. This is probably a result of the tendency of NDVI to overestimate high canopy density (Wang et al. 2010). While the limitation of NDVI to monitor subtle change in forest condition, it also allows the overall assessment of canopy condition across the landscape. For the California study area, the average predicted multi-scale decline using for the multi-scale model was 3.97, compared with NDVI of 5.12. The field-measured average for the region was 3.93. This indicates that a regional analysis using NDVI could potentially overestimate decline condition.

If the goal is to identify only and in moderate to severe decline, this may not be of concern. If, however, the goal is to identify early stage of decline, such as those associated with incipient infestation by spruce beetle and pathogens, the level of detail provided by the multi-scale model could be critical.

In a study of the cope of high-resolution comparison additional calibration techniques. In addition, the focus on the integration of aerial computed data could be obstructive and expensive for forest decline assessment. I recommend that future efforts to monitor forest decline consider this approach in order to maximize the information and accuracy possible with broadband sensor data available at this time.

4. Conclusions

The overarching goal of this study was to determine whether moderate and advanced assessment of canopy condition can be achieved using the commonly available multi-spectral imagery. This approach is unique in several ways: (1) the use of a detailed, continuous multi-scale decline using ground truth and model calibration; (2) consideration of narrow-band-derived vegetation indices adapted for broadband data; and (3) calibration with a multi-scale model designed to capture a range of decline symptoms. I found that forest condition could more accurately and consistently be predicted using a multi-scale prediction model than inclusion of narrow-band derived indices.

The final 5-element linear regression model is based on fitting narrow-band-derived vegetation indices known for their ability to chlorophyll content and function, canopy density, and moisture content. To my knowledge, these narrow-band indices have not been modified for multiple applications because of a widespread assumption that abundance features are degraded by the narrow-band wavelength combination and not detectable in the broadband image. While it is true that the original narrow-band indices are likely to measure a specific biophysical parameter for which they were designed, the overall indicator has been calculated using broadband data, information related to canopy conditions is gained in spite of a loss of spectral resolution.

References

- Adam, M. L., W. A. Noell, W. D. Philpot, and J. H. Peeler. 2000. "Spectral Detection of Micronutrient Deficiency in 'Bagg' Soybean." *Agronomy Journal* 92 (2): 261-268.

- Ca e, G. A., W. G. Cib la, and R. L. Mille . 1996. "Na o -Band Reflec ance Image Compa ed i h The mal Image fo Ea l De ec ion of Plan S e ." *Journal of Plant Physiology* 148 (5): 515–522. doi:10.1016/S0176-1617(96)80070-8.
- Ca e, G. A., and A. K. Knapp. 2001. "Leaf Op cal P ope ie in Highe Plan : Linking Spec al Cha ac e i ic o S e and Chlo oph ll Concen a ion." *American Journal of Botany* 88 (4): 677–684. doi:10.2307/2657068.
- Ca e, G. A., and R. L. Mille . 1994. "Ea l De ec ion of Plan S e b Digi al Imaging i hin Na o S e -Sen i ie Wa eband ." *Remote Sensing of Environment* 50 (3): 295–302. doi:10.1016/0034-4257(94)90079-5.
- Ca e, G. A., and B. A. Spie ing. 2002. "Op cal P ope ie of In ac Lea e fo E ima ing Chlo oph ll Concen a ion." *Journal of Environment Quality* 31 (5): 1424–1432. doi:10.2134/jeq2002.1424.
- Chande , G., B. L. Ma kham, and D. L. Helde . 2009. "S mma of Q en Radiome ic Calib a ion Coefficien fo Land a MSS, TM, ETM+, and EO-1 ALI Sen o ." *Remote Sensing of Environment* 113 (5): 893–903. doi:10.1016/j. e.2009.01.007.
- Cha Œ , P. S. 1988. "An Imp o ed Da k-Objec S b ac ion Techniq e fo A mo phe ic Sca eing Co ec ion of M l i pec al Da a." *Remote Sensing of Environment* 24: 459–479. doi:10.1016/0034-4257(88)90019-3.
- Chen, J. 1996. "E ak a ion of Vege a ion Indice and a Modified Simple Ra io fo Bo cal Applica ion ." *Canadian Journal of Remote Sensing* 22 (3): 229–242.
- Cho, M. A., and A. K. Skidmo e. 2006. "A Ne Techniq e fo Œ ac ing he Red Edge Po i ion fom H pe pec al Da a: The Linea Œ apola ion Me hod." *Remote Sensing of Environment* 101: 181–193. doi:10.1016/j. e.2005.12.011.
- D'Amb o io, N., K. Œ abo, and H. K. Lich en hale . 1992. "Inc ea e of he Chlo oph ll Fl o e cence Ra io F690/F735 Œ ing he A Œ mnal Chlo oph ll B eakdo n." *Radiation and Environmental Biophysics* 31 (1): 51–62. doi:10.1007/BF01211512.
- Da , B. 1998. "Remo e Sen ing of Chlo oph ll A, Chlo oph ll B, Chlo oph ll A + B, and To al Ca o enoid Con en in Œ cal p Œ Lea e ." *Remote Sensing of Environment* 66: 111–121. doi:10.1016/S0034-4257(98)00046-7.
- El idge, C. D., and R. J. P. L on. 1985. "E ima ion of he Vege a ion Con ib Œ ion o he 1.65/2.22 Œ m Ra io in Ai bo ne Thema ic Mape Image of he Vi ginia Range, Ne ada." *International Journal of Remote Sensing* 6 (1): 75–88.
- Gi el on, A. A., C. B Œ chmann, and H. K. Lich en hale . 1999. "The Chlo oph ll Fl o e cence Ra io F-735/F-700 a an Ac Œ a e Mea Œ e of he Chlo oph ll Con en in Plan ." *Remote Sensing of Environment* 69 (3): 296–302. doi:10.1016/S0034-4257(99)00023-1.
- Gi el on, A. A., and M. N. M Œ l ak. 1994. "

Ponikvar, J. and R. Halle. 2014. "

- Vieira, I. C. G., A. Silva de Almeida, E. R. Davidson, T. A. Stone, C. J. Reid, C. A. L. de Carvalho, and J. B. Grace. 2003. "Classifying Successional Forest Using Landsat Special Purpose and Ecological Characteristics in Eastern Amazonia." *Remote Sensing of Environment* 87: 470–481. doi:10.1016/j.rse.2002.09.002.
- Vogelmann, J. E., and B. N. Rock. 1988. "Assessing Forest Damage in High-Elevation Coniferous Forests in Vermont and New Hampshire Using Thematic Mapper Data." *Remote Sensing of Environment* 24 (2): 227–246. doi:10.1016/0034-4257(88)90027-2.
- Vogelmann, J. E., B. N. Rock, and D. M. Morel. 1993. "Red Edge Spectral Measurement from Sugar Maple Leaves." *International Journal of Remote Sensing* 14 (8): 1563–1575. doi:10.1080/01431169308953986.
- Wang, C., Z. Li, and T. L. Hu. 2007. "Using Landsat Images to Detect Oak Decline in the Mark Twain National Forest, Oak Highland." *Forest Ecology and Management* 240 (1–3): 70–78. doi:10.1016/j.foreco.2006.12.007.
- Wang, W. T., J. J. Qu, X. J. Hao, Y. Q. Li, and J. A. Santof. 2010. "Post-Hurricane Forest Damage Assessment Using Satellite Remote Sensing." *Agricultural and Forest Meteorology* 150 (1): 122–132. doi:10.1016/j.agrfor.2009.09.009.
- Williams, P., and K. Nozaki. 2001. *Near-Infrared Technology in the Agricultural and Food Industries*. St. Paul, MN: American Association of Cereal Chemists.
- Wolfe, P. T., and P. A. Townsend. 2011. "Multi-Sensor Data Fusion for Estimating Forest Species Composition and Abundance in Northern Minnesota." *Remote Sensing of Environment* 115 (2): 671–691. doi:10.1016/j.rse.2010.10.010.
- Wu, C., X. Han, Z. Ni, and J. Dong. 2010. "An Evaluation of EO-1 Hyper-Resolution Data for Chlorophyll Content and Leaf Area Index Estimation." *International Journal of Remote Sensing* 31: 1079–1086. doi:10.1080/01431160903252335.